Pivotal response treatment prompts a functional rewiring of the brain among individuals with autism spectrum disorder

Archana Venkataraman[a,b], Daniel Y.-J. Yang[c], Nicha Dvornek[b], Lawrence H. Staib[b], James S. Duncan[b,d], Kevin A. Pelphrey[e] and Pamela Ventola[c]

Behavioral interventions for autism have gained prominence in recent years; however, the neural-systems-level targets of these interventions remain poorly understood. We use a novel Bayesian framework to extract network-based differences before and after a 16-week pivotal response treatment (PRT) regimen. Our results suggest that the functional changes induced by PRT localize to the posterior cingulate and are marked by a shift in connectivity from the orbitofrontal cortex to the occipital–temporal cortex. Our results illuminate a potential PRT-induced learning mechanism, whereby the neural circuits involved during social perception shift from sensory and attentional systems to higher-level object and face processing areas. ***NeuroReport*** **27:1081–1085 Copyright © 2016 Wolters Kluwer Health, Inc. All rights reserved.**

NeuroReport 2016, **27:**1081–1085

Keywords: autism spectrum disorders, Bayesian analysis, functional MRI, pivotal response training

[a]Department of Electrical and Computer Engineering, Johns Hopkins University, Baltimore, Maryland, [b]Department of Radiology & Biomedical Imaging, Yale School of Medicine, New Haven Connecticut, [c]Center for Translational Developmental Neuroscience, Yale School of Medicine, New Haven Connecticut, [d]Department of Biomedical Engineering, Yale University, New Haven Connecticut and [e]Autism & Neurodevelopmental Disorders Institute, The George Washington University and the Children's National Health System, Washington, District of Columbia, USA

Correspondence to Archana Venkataraman, PhD, Department of Electrical and Computer Engineering, Johns Hopkins University, Baltimore, MD, 21218, USA Tel: +1 410 516 5704; e-mail: archana.venkataraman@jhu.edu

Received 11 July 2016 **accepted** 18 July 2016

Introduction

Autism Spectrum Disorders (ASDs) are characterized by social and communication deficits. Theories of ASD have postulated both reduced social motivation and atypical reward processing [1,2] as well as difficulty in predicting real-world events [3]. Given the universality of social deficits in ASD, dysfunctions in brain systems subservient to social perception are central to research in the field [4,5]. Moreover, core social-communication symptoms are natural targets for the development of pharmacological and behavioral interventions.

Behavioral therapies, such as pivotal response treatment (PRT) [6], have shown promise in reducing the core symptoms of ASD [7]. PRT is structured as a series of play-based sessions, during which children are reinforced for utilizing appropriate social-communication skills. Several randomized control trials of PRT have shown significant improvements in language and social functioning [8,9], and a recent open-label trial of PRT from our group showed a reduction in restricted and repetitive behavior following a 16-week PRT regimen [7].

Although it is believed that behavioral interventions for ASD stimulate socially responsive areas of the brain, little is known about the neural underpinnings of such therapies or their short-term and long-term effects on neural systems. To this end, Voos *et al.* [10] reported that two high-functioning children with ASD showed increased activation from baseline to treatment endpoint in key brain regions associated with social functioning. In a follow-up study, Ventola *et al.* [7] reported that the neural systems supporting social perception in an additional 10 children with ASD were malleable through implementation of PRT; specifically, neural responses were more similar to those of typically developing children following treatment. Using a similar treatment approach called the Early Start Denver Model (ESDM) [11], Dawson *et al.* [12] measured the neural correlates of response by electroencephalogram after 2 years of treatment. Following the intervention, children in the ESDM group showed a shorter Nc latency and increased cortical activation (decreased α power and increased θ power) when viewing faces compared with a group of children who received only a community-based intervention. This study, however, did not include a baseline time point; thus, it is not possible to evaluate whether and/or how the groups differed before the onset of ESDM treatment.

Understanding of the neural mechanisms of treatment response is crucial for mitigating the core social-communication deficits in ASD, from the development of novel and adaptive treatment approaches to behavioral and pharmacological therapies that target specific neural circuitries. Here, we leverage an unbiased probabilistic model for functional MRI (fMRI) that aggregates group-level changes in functional synchrony before and after treatment in order to localize a compact subset of affected regions, that is, treatment foci.

DOI: 10.1097/WNR.0000000000000662

Materials and methods

Participants

We studied 19 children with a primary diagnosis of ASD (age = 5.87 ± 1.09 years, 13 males). All participants were high functioning (intelligence quotient ≥ 70) and fulfilled the *Diagnostic and Statistical Manual of Mental Disorders*, 5th ed. (DSM-5) diagnostic criteria for ASD [13] by expert clinician judgment, as confirmed by the gold-standard Autism Diagnostic Interview-Revised [14] and the Autism Diagnostic Observation Schedule [15]. Further details of the patient demographics and clinical measures are provided in Table 1. Written informed consent was obtained from each set of parents and verbal assent was attained from each child. This study was approved by the Human Investigations Committee at Yale University and is registered at *www.ClinicalTrials.gov* (ID: NCT01908686).

Participants received 16 weeks of PRT [6,7], which involved 5 h of direct intervention with the clinician and 2 h of parental guidance at home per week. PRT is designed to increase the child's social motivation by naturalistic reinforcement and goal-oriented tasks. The sessions were play based and targeted pivotal behaviors, such as social initiation and responsiveness. It is believed that improvements in these domains will lead to more widespread and generalized improvements across development. All clinicians involved in the present study were extensively trained in PRT. Fidelity was maintained by videotaping and reviewing randomly selected time intervals during each patient's sessions. Overall, this sample represents 2128 h of direct therapeutic intervention, 1064 family visits, and 57 clinical evaluations, in addition to the MRI protocol, as described below.

Image acquisition and preprocessing

Each child underwent MRI scanning before and after the PRT intervention. Participants were scanned on a Siemens MAGNETOM 3 T Tim Trio scanner (Siemens Medical Solutions, Erlangen, Germany) at Yale. We acquired a T1-weighted scan (MP-RAGE, TR = 1900 ms, TE = 2.96 ms, flip angle = 9°, resolution = 1 mm^3 and an fMRI scan (BOLD, TR = 2000 ms, TE = 25 ms, flip angle = 60°, resolution = $3.44 \times 3.44 \times 4$ mm^3) for each patient.

Table 1 Snapshot of participant demographics and clinical characteristics (19 patients)

Variable	Mean (SD)
Pretreatment age (years)	5.87 (1.09)
Sex: male (0 = female, 1 = male)	0.68 (0.48)
DAS-II General conceptual ability (IQ)[a]	104.53 (16.78)
Handedness (1 = right, 0 = ambi, −1 = left)	0.68 (0.67)
ADOS (Calibrated Severity Score)	7.74 (2.13)
CELF-P-2 core language[a]	91.32 (24.18)
Pretreatment SRS-parent total raw score	81.68 (22.65)
Post-treatment SRS-parent total raw score	66.53 (23.52)
Pretreatment head motion (mm)	1.38 (1.35)
Post-treatment head motion (mm)	0.46 (0.44)

Note: Treatment outcome is the residual change in the SRS-parent total raw score, that is, the δ change (post − pre) minus the predicted change, as specified by the group-wise linear trend.
ADOS, Autism Diagnostic Observation Schedule; DAS-I, Differential Ability Scales-II; IQ, intelligence quotient; SRS, Social Responsiveness Scale.
[a]Standard Score.

The fMRI paradigm featured coherent and scrambled point-light animations, presented in an alternating block-design framework (24 s per block). The coherent biological motion shows a point-light figure performing movements relevant to early childhood experiences [4]. Scrambled animations combine the trajectories of 16 randomly selected points from the coherent displays.

We processed the anatomical images using Freesurfer [16]. Region boundaries were derived from the built-in Desikan–Killany atlas, which segments the brain into 86 cortical and subcortical regions, roughly corresponding to Broadmann areas. The fMRI data were preprocessed using FSL, v5.0.8 [17] according to the processing steps outlined by the creators of ICA-AROMA [18]. The pipeline consists of the following steps: (a) motion correction using MCFLIRT, (b) interleaved slice timing correction, (c) BET brain extraction, (d) global mean intensity normalization for the entire 4D data set, (e) spatial smoothing with full width at half maximum = 5 mm, (f) denoising with ICA-AROMA [18], (g) nuisance regression of white matter and cerebrospinal fluid signals to remove physiological noise, and (h) high-pass temporal filtering. The first four volumes were discarded and preprocessed data were then prewhitened using FSL FILM to remove time-series autocorrelation. Both the functional and the anatomical data were registered to the MNI152 standard brain for subsequent analysis. The pairwise fMRI measures are computed as the Pearson correlation coefficients between the mean time courses of the two regions. We center the correlation distribution of each patient to model relative deviations from the patient-specific baseline functional synchrony.

Bayesian analysis

Unlike traditional connectomics, which compares either pairwise correlation coefficients or average node-based measures between groups [19], our framework explicitly models the altered network topology while simultaneously adapting to both noise and patients variability [20,21]. Within a Bayesian setting, we estimate a latent or a hidden graph that characterizes the spread of altered functional connectivity from the region foci. This latent template subsequently explains the observable differences in fMRI correlation values. Hence, our model effectively translates connectivity information into estimates of the brain regions associated with PRT. Our approach is completely data-driven and does not impose spatial constraints on the region foci or altered functional pathways. By examining brain activity during a social perception task, we focus on functional connectivity during social information processing, a key area of deficit in individuals with ASD and target of PRT.

We consider two forms of model validation. First, we evaluate the reliability of the detected region foci by bootstrapping. Bootstrapping is a statistical technique, by which we subsample the data to derive robust estimates of a given model characteristic (e.g. the network foci). In this work, we infer the model parameters while omitting either one or two patients from the analysis. By aggregating the network results across subsets of the patient cohort, we can speculate on the generalizability of our network results for potentially larger PRT datasets. Second, we regress the post-treatment fMRI correlation values implicated by the inferred Bayesian network with the residualized change in Social Responsiveness Scale (SRS) [22] before and after PRT. SRS was the primary outcome measure for our clinical trial and provides a link between our neuroimaging markers and the behavioral improvement observed.

Results

Figure 1 shows the model results when comparing the pretreatment and post-treatment functional synchrony across the scrambled and coherent biological motion conditions. As can be seen, the aggregate differences localize to the posterior cingulate cortex (PCC), depicted in yellow. We also observe a reduction in connectivity to orbital frontal cortex (blue) as well as an increase in connectivity to the occipital–temporal cortex (magenta).

Figure 2a highlights the selection frequency of each cortical area across the 19 unique leave-one-out (excluding roughly 5% of the data) subsets and 171 unique leave-two-out subsets (excluding roughly 10% of the available data). Despite the small sample size, our region foci consistently localize to the PCC on the basis of 18 patients and to either the PCC or the frontal cortex on the basis of only 17 patients. These findings indicate that almost all identifiable networks were centered on the PCC. This reproducibility further strengthens the clinical relevance of our results.

Figure 2b reports the connections with the largest coefficients of determination (R^2) values. Although our sample size was too small to test the significance of these correlations, the effect sizes are encouraging and suggest that the networks that we identified are related to the therapeutic processes engaged by PRT.

Discussion

It is striking that the PRT-induced changes in connectivity involve both a reduction in connectivity between the PCC and the orbital frontal cortex and an increase in connectivity between the PCC and regions of the ventral occipital–temporal extrastriate cortex. The PCC is well known for its roles in social cognition [23]. The orbital frontal cortex is generally implicated in assessing the reward value of stimuli in the environment [1]. In contrast, sectors of the ventral occipital and temporal cortex are well known for processing various socially meaningful stimuli including faces and biological motion [24]. PRT seems to facilitate a process by which the brain shifts from a strong reliance on an orbital frontal–PCC circuit to a PCC–ventral occipital–temporal cortex circuit [7].

Fig. 1

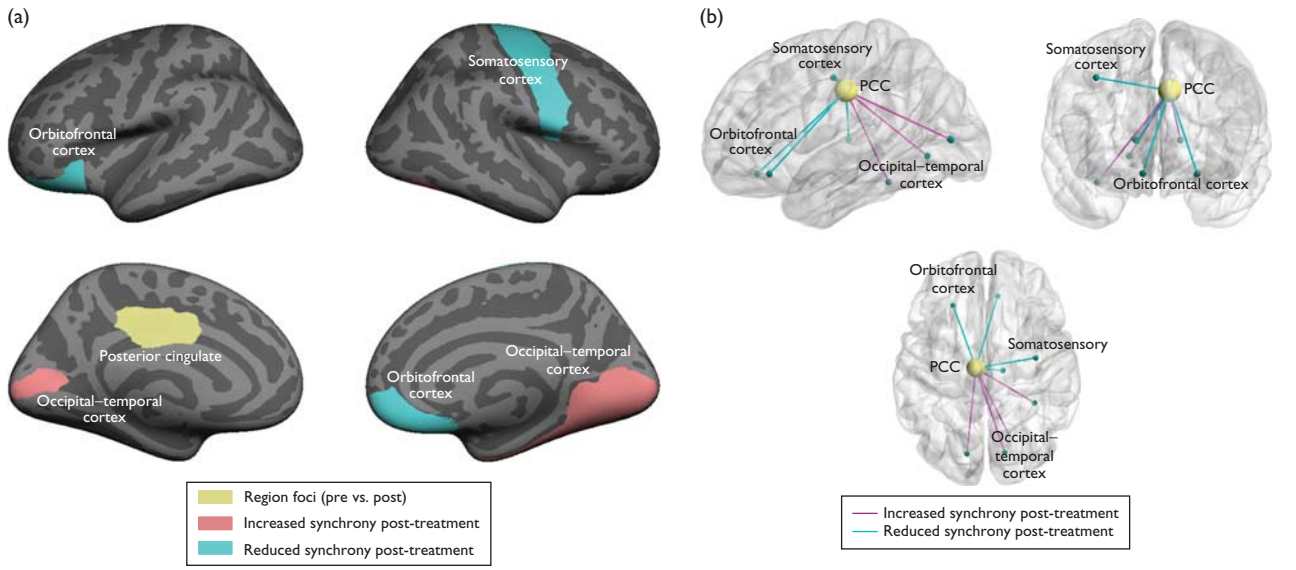

Network differences before (pre) and after (post) the 16-week PRT regimen. (a) Region membership in the altered network. The functional differences localize to the posterior cingulate (yellow). The pink and blue areas indicated increased and reduced functional synchrony to the PCC after treatment. (b) 3D diagram of the altered functional synchrony. Each node corresponds to one of the predefined regions and each edge represents a functional connection. Blue lines signify reduced functional synchrony after treatment; magenta lines indicate increased functional synchrony. PCC, posterior cingulate cortex; PRT, pivotal response treatment.

Fig. 2

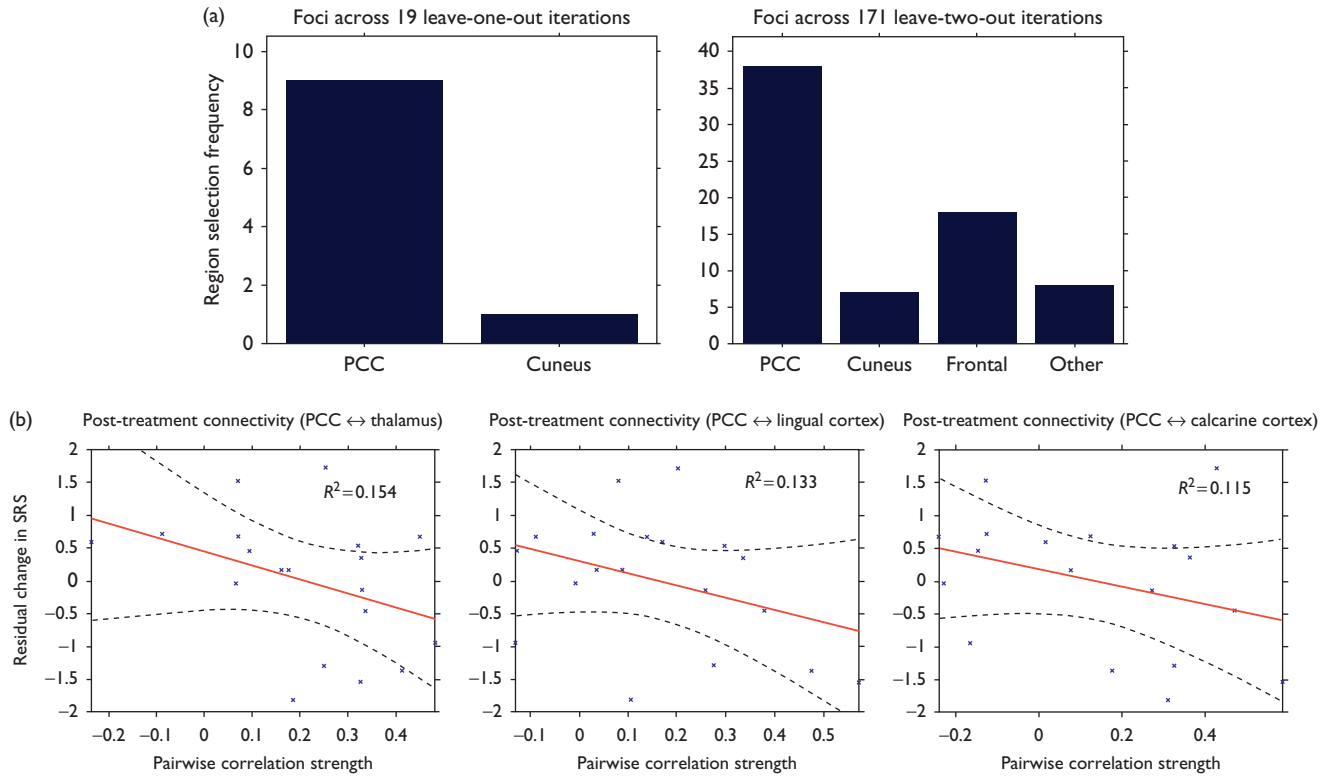

Model validation for the PRT analysis. (a) Reproducibility of the region foci on excluding one (left) and two (right) patients from the analysis. Results are aggregated across all 19 and 171 bootstrapping configurations, respectively. (b) Linear regression between the pairwise functional MRI correlation values and the residual change in SRS. The patient data are plotted in blue, and the linear fit and confidence intervals are overlaid in red and black, respectively. PRT, pivotal response treatment; SRS, Social Responsiveness Scale.

Our conclusions are also supported by the broader fMRI literature, as cataloged by the Neurosynth meta-analytic database (*http://www.neurosynth.org*). Broadly, Neurosynth aggregates both the spatial activation coordinates and the psychological words and phrases used to describe these effects across nearly 10 000 published fMRI studies. The web-based system leverages the power of large datasets to compute whole-brain posterior probabilities ($P_{\text{featurel coordinate}}$) for individual psychological terms at each spatial coordinate [25]. Figure 3 shows the top eight 'features' implied by the regions with increased (pink) and reduced (blue) synchrony to the posterior cingulate after PRT. As can be seen, there is a general shift from sensory topics, such as eye, movement, and finger to higher-level constructs, such as scene, identity, and face recognition. Hence, our results seem to support a PRT-induced social learning process by which children with ASD initially rely on motivational and attentional systems during social perception, as indicated by the preponderance of connectivity with the orbital frontal cortex. Following PRT, social perception begins to engage higher-level systems involved in the recognition and classification of both social and nonsocial objects, supported by regions of the temporal–occipital cortex.

These PRT-induced changes in connectivity are the first steps toward the goal of targeted, precision medicine for core social-communication deficits in ASD. As a whole, the work toward precision medicine in ASD has been hindered by a lack of sensitive, objective biomarkers of treatment response. By objectively illustrating changes in connectivity and by revealing the key neuroanatomical circuits implicated in response to treatment, we are providing the crucial and much-needed foundation to individualized treatment approaches and the development of novel/adaptive treatments that target specific neural circuits. Furthermore, these biological markers can be used toward the development of objective early efficacy indicators of treatment response. In time, these neural systems-based biomarkers may also be tied to behavioral indicators, which will increase the scalability of the proposed treatment approach.

Despite the significance of the results presented here, there are clear limitations. The sample size, although consistent with other behavioral trials of children with ASD, is small. In addition, we did not have a typically developing control group for comparison. Nonetheless, the results are highly impactful and among the first to

Fig. 3

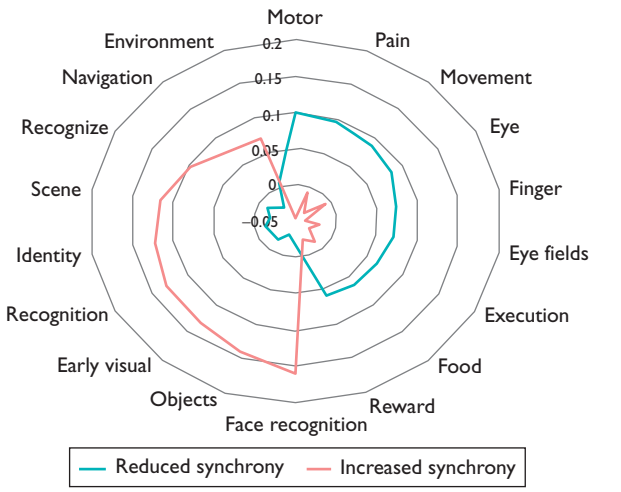

Specificity of neurocognitive functions derived from the Neurosynth meta-analytic database. Blue corresponds to the regions with reduced synchrony to the posterior cingulate after PRT. The constructs implicate basic sensory functions. Magenta indicates the regions with increased synchrony to the posterior cingulate and maps onto scene and object-recognition domains. PRT, pivotal response treatment.

show changes in connectivity following treatment for ASD.

Acknowledgements

Funding for the PRT study was provided by the Autism Science Foundation, the Simons Foundation, the Women's Health Research at Yale, the Deitz Family, Esme Usdan & Family, and the Dwek Family. The analysis was supported in part by R01 NS035193 (NINDS), R01 MH100028 (NIMH) and the Yale Biomedical High Performance Computing Center (NIH RR19895 and RR029676-01). D. Yang is also supported by the Autism Speaks Meixner Postdoctoral Fellowship in Translational Research (#9284).

Author contributions: A.V. developed the Bayesian network model, analyzed the PRT data, generated the figures, and drafted the manuscript; D.Y. preprocessed the fMRI data and obtained the Neurosynth results; K.A.P. and P.V. participated in the design of the study and helped to draft the manuscript; N.D., L.H.S., and J.S.D. facilitated the research and discussion. All authors have read and approved the final document.

Conflicts of interest

There are no conflicts of interest.

References

1 Scott-Van Zeeland AA, Dapretto M, Ghahremani DG, Poldrack RA, Bookheimer SY. Reward processing in autism. *Autism Res* 2010; **3**:53–67.
2 Pelphrey KA, Yang DYJ, McPartland JC. Building a social neuroscience of autism spectrum disorder. *Curr Top Behav Neurosci* 2014; **16**:215–233.
3 Sinha P, Kjelgaard MM, Gandhi TK, Tsourides K, Cardinaux AL, Pantazis D, *et al.* Autism as a disorder of prediction. *Proc Natl Acad Sci USA* 2014; **111**:15220–15225.
4 Kaiser MD, Hudac CM, Schultz S, Lee SM, Cheung C, Berken AM, *et al.* Neural signatures of autism. *Proc Natl Acad Sci USA* 2010; **107**:21223–21228.
5 Dawson G, Webb SJ, McPartland J. Understanding the nature of face processing impairment in autism: insights from behavioral and electrophysiological studies. *Dev Neuropsychol* 2005; **27**:403–424.
6 Koegel RL, Schreffirnan L, Good A, Cerniglia L, Murphy C, Koegel LK. *How to teach pivotal behaviors to children with autism: a training manual*. San Diego, CA: UC Graduate School of Education; 1989.
7 Ventola P, Friedman HE, Anderson LC, Wolf JM, Oosting D, Foss-Feig J, *et al.* Improvements in social and adaptive functioning following short-duration (PRT) program: a clinical replication. *J Autism Dev Disord* 2014; **44**:2862–2870.
8 Hardan AY, Gengoux GW, Berquist KL, Libove RA, Ardel CM, Phillips J, *et al.* A randomized controlled trial of pivotal response treatment group for parents of children with autism. *J Child Psychol Psychiatry* 2015; **58**:884–892.
9 Mohammadzaheri F, Koegel LK, Rezaee M, Rafiee SM. A randomized clinical trial comparison between pivotal response treatment (PRT) and structured applied behavior analysis (ABA) intervention for children with autism. *J Autism Dev Disord* 2014; **44**:2769–2777.
10 Voos AC, Pelphrey KA, Tirrell J, Bolling DZ, Vander Wyk B, Kaiser MD, *et al.* Neural mechanisms of improvements in social motivation after pivotal response treatment: two case studies. *J Autism Dev Disord* 2013; **43**:1–10.
11 Princiotta D, Goldstein S. Early start Denver model: an intervention for young children with autism spectrum disorders. In: Sam Goldstein, Jack A. Naglieri, editors. *Interventions for autism spectrum disorders: translating science into practice*. New York, NY: Springer; 2013. pp. 59–73.
12 Dawson G, Jones EJ, Merkle K, Venema K, Lowy R, Faja S, *et al.* Early behavioral intervention is associated with normalized brain activity in young children with autism. *J Am Acad Child Adolesc Psychiatry* 2013; **51**:1150–1159.
13 American Psychiatric Association. *Diagnostic and Statistical Manual of Mental Disorders*. Arlington, VA: American Psychiatric Publishing; 2013.
14 Lord C, Rutter M, Le Couteur A. Autism diagnostic interview-revised: a revised version of a diagnostic interview for caregivers of individuals with possible pervasive developmental disorders. *J Autism Dev Disord* 1994; **24**:659–685.
15 Lord C, Risi S, Lambrecht L, Cook EH, Leventhal BL, di Lavore PC, *et al.* The autism diagnostic observation schedule-generic: a standard measure of social and communication deficits associated with the spectrum of autism. *J Autism Dev Disord* 2000; **30**:205–223.
16 Fischl B, Salat D, van der Kouwe AJ, Makri N, Segonne F, Quinn BT, Dale AM. Sequence-independent segmentation of magnetic resonance images. *NeuroImage* 2004; **23**:69–84.
17 Smith SM, Jenkinson M, Woolrich MW, Beckmann CF, Behrens TE, Johansen-Bern H, *et al.* Advances in functional and structural MR image analysis and implementation as FSL. *NeuroImage* 2004; **23** (Suppl 1): 208–219.
18 Pruim RH, Mennes M, van Rooij D, Llera A, Buitelaar JK, Beckmann CF. ICA-AROMA: a robust ICA-based strategy for removing motion artifacts from fMRI data. *NeuroImage* 2015; **112**:267–277.
19 Di Martino A, Yan CG, Li Q, Denio E, Castellanos FX, Alaerts K. The autism brain imaging data exchange: towards a large-scale evaluation of the intrinsic brain architecture in autism. *Mol Psychiatry* 2014; **19**:659–667.
20 Venkataraman A, Kubicki M, Golland P. From brain connectivity models to region labels: identifying foci of a neurological disorder. *IEEE Trans Med Imaging* 2013; **32**:2078–2098.
21 Venkataraman A, Duncan JS, Yang D, Pelphrey KA. An unbiased Bayesian approach to functional connectomics implicates social-communication networks in autism. *NeuroImage Clin* 2015; **8**:356–366.
22 Constantino JM. *Social Responsiveness Scale*, 2nd ed. Torrance, CA: WPS; 2012.
23 Buckner RL, Andrews-Hanna JR, Schacter DL. The brain's default network anatomy, function, and relevence to disease. *Ann NY Acad Sci* 2008; **1124**:1–38.
24 Schultz RT, Gauthier I, Klin A, Fulbright RK, Anderson AW, Volkmar F, *et al.* Abnormal ventral temporal cortical activity during face discrimination among individuals with autism and Asperger syndrome. *Arch Gen Psychiatry* 2000; **57**:331–340.
25 Yarkoni T, Poldrack RA, Nichols TE, van Essen DC, Wagner TD. Large-scale automated synthesis of human functional neuroimaging data. *Nat Methods* 2011; **8**:665–670.